

## The Relation between Non-adipose Muscle Fat and Hepatic Steatosis Studied with Localized <sup>1</sup>H Magnetic Resonance Spectroscopy (<sup>1</sup>H MRS) and LC-MS Techniques

van Ginneken VJT<sup>1\*</sup>, Ronald Booms<sup>2</sup>, Elwin Verheij<sup>3</sup>, Evert de Vries<sup>1</sup> and Jan van der Greef<sup>3,4</sup>

<sup>1</sup>Blue Green Technologies, Runderweg 6, 8219 PK, Lelystad, Netherlands

<sup>2</sup>Department of Aquaculture and Fisheries, 6700 AH Wageningen, Netherlands

<sup>3</sup>TNO Pharma, 3700 AJ Zeist, Netherlands

<sup>4</sup>Sino-Dutch Center for Preventive and Personalized Medicine, Leiden University, 2300 RA Leiden, Netherlands

### Abstract

**Aim/objective:** In this study we investigated ectopic fat storage in the muscle and the liver using <sup>1</sup>H Magnetic Resonance Spectroscopy (<sup>1</sup>H-MRS). The inability to store fat in adipose tissue leads to ectopic Triacylglycerol (TG) accumulation in muscle followed by the liver: the so called “overflow hypothesis”. It is assumed that when steatosis occurs in organs like the liver we can speak from “Metabolic Syndrome”.

**Methods:** We compared the effects of two different diet interventions, 24 h-starvation and 40 days High-fat diet (+0.25% cholesterol and 45% energy from bovine lard) with control mice. Characterization of lipid molecular species in non-adipose muscle homogenate was performed by comparing the groups using liquid chromatography coupled to mass spectrometry (LC-MS) techniques following a Systems Biology lipidomics based approach. Reversed phase liquid chromatography coupled to mass spectrometry (LC-MS) were used to quantify and qualify the rearrangement and repartitioning of the triacylglycerol compound in the liver organ.

**Results:** The major message of this manuscript is the interaction of remnant organ/tissue called “carcass” in the absorption capacity of lipids and the spill-over of these lipid compounds (mainly TG’s) to the liver. Our data suggest that if the remnant muscle compartment is saturated with lipids until ≈500 g/kg dry matter there is no TGs accumulation in the liver, but above this level there is a spill over in the plasma resulting in fat accumulation in the liver.

**Conclusion:** We demonstrated in this study that fat can be stored in the muscle but when this compartment is saturated the liver takes over the function as a fat sink, the “overflow hypothesis” resulting finally in hepatic steatosis and ‘Metabolic Syndrome’.

**Keywords:** Lipids; Carcass; Non-adipose muscle fat; High-fat diet; Starvation; C57bl6 mouse model; LC-MS; <sup>1</sup>H MRS

### Introduction

Glucose homeostasis is a physiologically well-balanced mechanism depending on three coordinated and simultaneously ongoing processes involving insulin secretion by the pancreas, hepatic glucose output and glucose uptake by splanchnic (liver and gut) and peripheral tissues (muscle and fat) (Figure 1) [1,2]. Under normal circumstances, glucose is the only fuel the brain and nerve cells can use [3,4] but also erythrocytes exemplify such glucose-dependent cells [4]. Furthermore glucose is also a preferred substrate by muscle during the initial stages of exercise [5]. This complicated interaction between the different organs/tissues in terms of maintaining overall or more specific organ/tissue energy homeostasis is indicated with the word “crosstalk” [6]. This interaction between organs is also observed under conditions of starvation [7-9]. This “crosstalk” with as major regulator hormones insulin and glucagon is depicted in Figure 1. A dysregulation may lead to the pathogenesis of Insulin resistance (IR) and/or Type-2 diabetes (T2DM). With respect to the partitioning between glucose and fatty acids as substrates in muscle tissue it was demonstrated that the relationship between glucose and fatty acids is integrated and reciprocal termed “metabolic flexibility” and that (mainly under conditions of starvation) muscle prefers fatty acids and mechanisms exists under starvation conditions to restrict glucose metabolism [10]. However, under conditions of obesity and IR/T2DM the metabolic flexibility is impaired, resulting an impaired switching from fatty acids

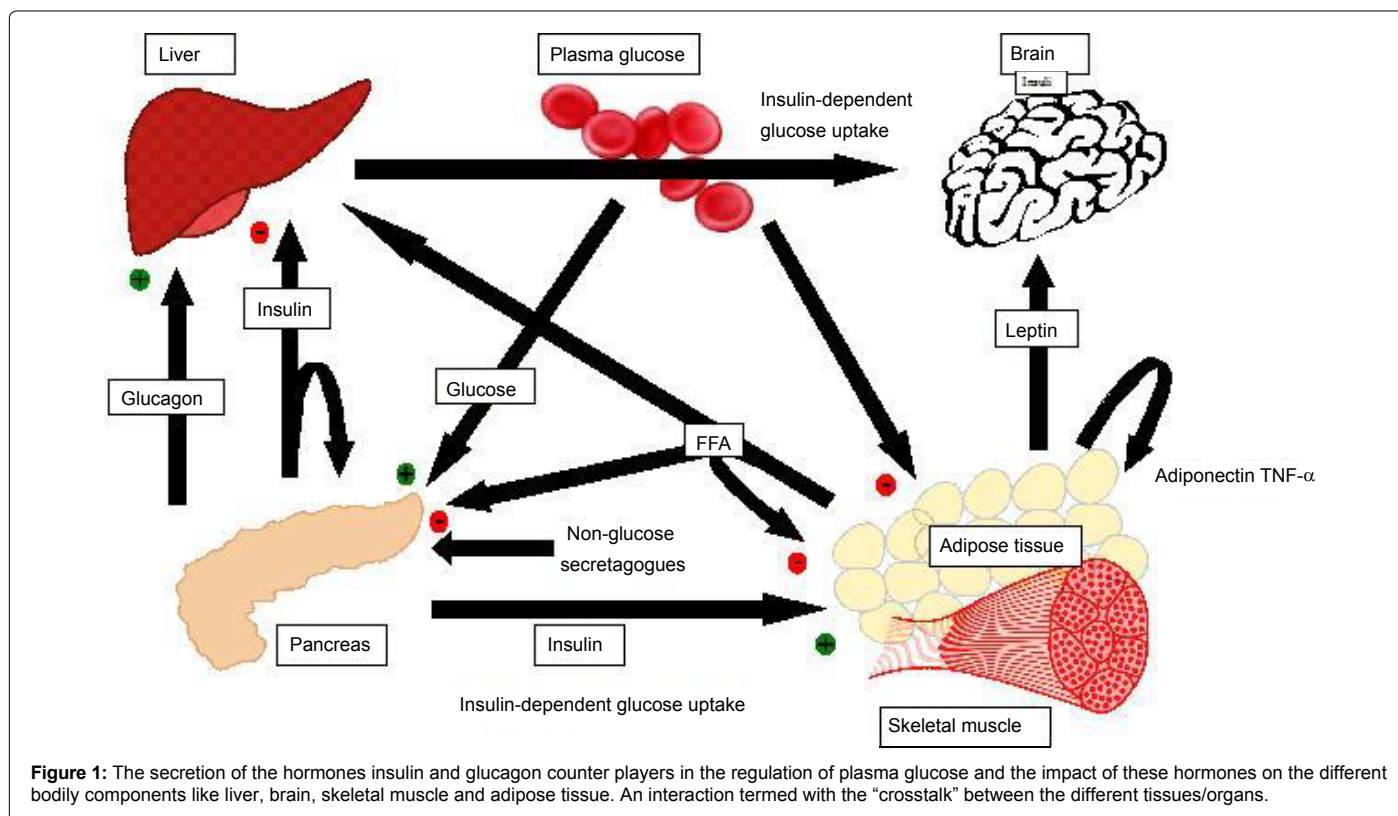
to glucose in response to insulin which has the consequence that blood glucose will increase [11]. Chavez and Summers [12] gave a review of the effects of accumulation of fat in peripheral tissues not suited for lipid storage. This has deleterious consequences on organ function, leading to cellular damage that underlies T2DM, heart disease [13], and hypertension. They hypothesize that the metabolic diseases associated with obesity, including T2DM and cardiovascular disease, derive from a common pathogenesis characterized of two independent stages: a). Selective IR; and b). Lipotoxicity which means the accumulation of fat in tissues not suited for lipid storage like common muscle or hearth muscle which has deleterious consequences on organ function, leading to cellular damage that underlies chronic inflammatory diseases like e.g. T2DM [12]. In healthy lean subjects muscle (lust like brain, [14])

**\*Corresponding author:** van Ginneken VJT, Blue Green Technologies, Runderweg 6, 8219 PK, Lelystad, Netherlands, Tel: 31(0)638071180; E-mail: [vwanginneken@hotmail.com](mailto:vwanginneken@hotmail.com)

**Received** August 30, 2016; **Accepted** September 26, 2016; **Published** October 02, 2016

**Citation:** van Ginneken VJT, Booms R, Verheij E, de Vries E, van der Greef J (2016) The Relation between Non-adipose Muscle Fat and Hepatic Steatosis Studied with Localized <sup>1</sup>H Magnetic Resonance Spectroscopy (<sup>1</sup>H MRS) and LC-MS Techniques. *Anat Physiol* 6: 245. doi: [10.4172/2161-0940.1000245](https://doi.org/10.4172/2161-0940.1000245)

**Copyright:** © 2016 van Ginneken VJT, et al. This is an open-access article distributed under the terms of the Creative Commons Attribution License, which permits unrestricted use, distribution, and reproduction in any medium, provided the original author and source are credited.



has a preference for glucose as substrate but giving a High-fat diet it is hypothesized that muscle fibers adjust to utilize calorically dense fatty acids, rather than glucose, as a primary energy source [12]. However, insulin stimulated lipogenesis, particularly in the liver and adipose tissue is unaltered or enhanced. This selective IR is one of several factors which predispose individuals to cardiovascular disease and T2DM [15,16]. During IR muscle is adapting to oxidize lipids, while sparing glucose which results in an increased concentration of glucose in the blood plasma, a characteristic of T2DM. Also selective IR resulting in elevation of intracellular lipid metabolites. The pathogenesis of IR/T2DM among humans is complex and is besides nutritional and lifestyle factors dependent on others like gender, ethnic group, age and (evolutionary determined) genetic susceptibility [9].

Mouse models have provided exciting novel observations and insight in the relation between hyperlipidemia, insulin resistance and obesity. In mice, in principle, fat cells can be isolated from four adipose pools: retroperitoneal, epididymal, mesenteric and subcutaneous [17]. However, little information is available about the role of fat from non-adipose tissue stores like intramuscular fat in relation to organs like the liver. An important goal of our research is to determine the interaction between the different fat pools in the development of obesity. In the relationship between RMR and organ morphology in mice the most significant morphological trait linked to differences in RMR is the liver [18]. The processes of fat accumulation in the liver are regulated via processes at the ‘input-side’: hepatic TG uptake dependent on the influx of Free Fatty Acids (FFA), fatty acid synthesis, and esterification. The three main sources of hepatic Fatty Acids available for TG formation are dietary fat, adipose fat, and fatty acid synthesis in the liver. Furthermore, removal of fat from the liver is also regulated via processes affecting the ‘output’ side: TG export as very-low-density lipoprotein (VLDL) or its oxidation to CO<sub>2</sub>, H<sub>2</sub>O and/or

ketones [19]). A major cause for hepatic steatosis is increased fatty acid flux to the liver caused by a high availability of plasma FFA in relation to peripheral oxidative requirements. This process can be observed under a condition of High-fat feeding as a result of a saturation of the muscle ‘storage’ compartment. The assignment of dietary energy above maintenance to lipid accretion in growing mice is largely determined by the relationship between fat intake and protein deposition. Little is known about the interaction between body composition (fat free mass: ash, protein and water) under conditions of excess fat overfeeding normal growth or starvation. Also the effect of fat overfeeding and starvation on subsequent protein and lipid deposition, however, is unclear. The second aim of this investigation was therefore to study the relationships between fat intake and starvation on the deposition of lipids and catabolism in the carcass in growing mice (20-35 g) as affected by previous nutrition or starvation.

The dynamics of lipid accumulation in the liver of a mouse model in relation to body fat carcass after a period of a High-fat diet are largely unknown. We hypothesize that fat can be stored in the muscle compartment but when this compartment is saturated the liver takes over the function as a fat sink, the “overflow hypothesis” resulting finally in ‘Metabolic Syndrome’. The major aim of this study was therefore to make a correlation between carcass fat concentration and TG accumulation in the liver of a mouse model *in vivo* after a period of a 40 days period of a High-fat diet, using non-invasive localized proton <sup>1</sup>H-MRS.

## Material and Methods

### Experimental set up

Male, 12-16 weeks old C57Bl/6 mice obtained from Charles River (Maastricht, Netherlands (N=50)) were used in all experiments. Mice

were housed in a temperature-controlled room (23°C) on a 10-hour dark/14-hour light cycle and had free access to standard mouse chow and water. All animal experiments were approved by the Animal Authorization Committee of Leiden University Medical Center (The Netherlands) which meets the demands as described by Fawcett [20]. To meet the requirements of the Code of Practice (Guideline 22: guidelines for the housing of mice in scientific institutions) that is to provide accommodation that meets the species specific needs of mice), housing should allow mice the opportunity for social interaction, the opportunity to carry out normal behaviors and the opportunity to rest and withdraw from each other. Normal behaviors of mice include eating, drinking, urinating, defecating, foraging, exploring, gnawing, hiding, climbing, playing, nesting, digging and engaging in a range of social activities. Three amounts of number of mice were used for the three different performed experiments described within the experimental protocol. In addition, all 50 animals were sacrificed in the several experiments. For sampling whole tissues and carcass the animals were sacrificed with an overdose of the anaesthesia isoflurane. Three different performed experiments described within the experimental protocol.

**MRS experiment:** 30 mice: N=14 Control, N=15 High-fat diet exposed, N=1 individual followed during exposure period of 40 days to High-fat diet.

**LC-MS-measurements:** Twenty mice were randomly assigned to one of three treatments. Treatment A: the Control group (n=6) and received ad-lib standard lab chow and water during 40 days. During Treatment B: animals were deprived from food for 24 hours (n=7). Treatment C: were animals that received a High-fat diet during 40 days (n=7).

**Carcass-analysis:** (Allometry) The same animals like under 2: LC-MS measurements: Control (N=6); Starvation (24 hours starvation, N=7); High-fat diet (40 days, N=7).

## Diet

Mice were fed a standard lab chow (SDS.3, Special Diet Services, Witham, UK) which contained about contained 22.4% protein, 4.3% fat (based on crude oil), 51.2% carbohydrates, 4.2% fibers, 7.6% minerals, 10% moisture (weight-percentages) and 0.0 % cholesterol. In contrast, the High-fat diet (Arie Blok, food code 4032.05, Woerden, The Netherlands) contained 21.4% protein, 36.2% carbohydrates, 24.0% fat (based on bovine lard), 6.2% fibers, 2.3% minerals, 5.74% moisture (weight-percentages) and 0.25% cholesterol. Mice were fasted 4 hours before the experiment to standardize their metabolic rate. The diets contained approximately the same caloric content: Standard 17-kJ/ g dm vs. High-fat diet 21-kJ/ g dm (Table 1). During the experiment the Control mice and High-fat mice were provided unrestricted amounts of food and water. The 24 hr starvation mice were given water *ad libitum*. To standardize the metabolic rate of the different mice groups they were fasted 4 hours before the start of the experiment.

For a further description of the Control Chow (SDS.3) and High-fat diet (4032.05) for:

i) Lipid composition determined with LC-MS techniques (the different lipid fraction like Phosphatidylcholine (PC), Sphingomyelin (SPM), Lysophosphatidylcholine (LPC), Cholesterylesthers (ChE) and Triacylglycerols (TG).

ii) The calculated Saturation Index for these lipid compounds.

iii) 3-D images for the food composition [14].

## Tissues

After measuring a voxel of the liver *in vivo* in the Bruker 9.4 Tesla magnet, the liver was removed in the anaesthetized animal. A tissue homogenate (~10% wet weight/vol) in PBS (phosphate-buffered saline) was made by stirring the tissue in a closed tube with small glass globules. For the carcasses the head including brain was removed, tail, legs, all abdominal tissues and organs and adipose fat was removed. The skin including subcutaneous fat was removed. As a result only a remaining carcass, remnant muscle indicated with “spare rib” was left. From this remnant muscle (carcass) a sample was taken and prepared for LC-MS measurements as described.

## Experimental Set Up

### Experiment 1: <sup>1</sup>H-MRS-test

Male, 12-16 weeks old C57Bl/6 mice (Ntotal=30) were housed in a temperature-controlled room (21°C) on a 10-hour dark/14-hour light cycle. Before the experiment started all animals had unrestricted access to food and water. Three treatments were compared: Treatment A.) (Control, n=14) received ad libitum standard mouse chow (SDS.3, Special Diet Services, Witham, UK) and water; Treatment B.) (n=15) ad an ad-lib High-fat diet (4032.05, Arie Blok, Woerden, The Netherlands) and water. C.) (n=1), an individual mouse was followed during the exposure period of 40 days on a High-fat diet and neutral lipid resonances measured *in vivo* in liver tissue of this individual black-six mouse were measured at: t=0, t=18, t=28, t=40 days using localized <sup>1</sup>H-MRS spectroscopy. Only the water peak at 4.6 ppm and the triacylglycerol (TG) peak at 1.2 ppm were followed in this same animal. In this was with non-invasive <sup>1</sup>H-MRS technique this animal serves as its own control.

**Anesthetizing of individual mouse during *in vivo* localized <sup>1</sup>H-magnetic resonance spectroscopy:** For liver imaging [14], the 30 mice were treated in the following way. As remarked from pilot experiments we observed that we were unable anesthetizing the 24 h starvation mice. Anaesthetizing of each individual mice of the High-fat diet group (N=15) or Control group (N=14) and the “time-followed” animal (N=1) was performed by exposing each animal to 4% isoflurane in air (50%) and O<sub>2</sub> (50%) and anesthesia was maintained with ~1.5% isoflurane. All images and spectra were respiration-gated using an air-pressure cushion connected to a laptop using Biotrig software (Bruker, Rheinstatten, Germany). Anesthesia depth was constantly regulated to maintain a stable respiration rate during the experiment. *In vivo*

Proximate Analysis	Control Chow (SDS.3)	Proximate Analysis	High-fat diet (4032.05)
Moisture (%)	10.00	Moisture (%)	5.74
Crude Oil (%)	4.25	Crude Fat (Bovine Lard) (%)	24.00
Crude Protein (%)	22.39	Crude Protein (%)	21.44
Crude Fiber (%)	4.21	Crude Fibre (%)	6.16
Minerals	7.56	Minerals	2.25
Nitrogen Free Extract	51.20	Nitrogen Free Extract	36.19
-----	-	Cholesterol	0.25
TOTAL	99.61	TOTAL	96.03
Measured Energy (Bombcalorimetry, [kJ/g dm])	16.86	Measured Energy (Bombcalorimetry, [kJ/g dm])	21.46

**Table 1:** Food constitution of the mice chow: “Normal Chow” for the Control group (Special Diet Services, SDS No.3, Witham, UK) and the High-fat diet (Arie Blok, food code 4032.05, Woerden, The Netherlands) based on bovine lard and 0.25% cholesterol.

<sup>1</sup>H MRS localized spectroscopy was carried out on a 9.4 T vertical bore imaging system equipped with an Avance console controlled by ParaVision 3.01 software, Bruker Biospin (Karlsruhe, Germany). For sampling whole tissues and carcass the animals were sacrificed with an overdose of the anesthesia isoflurane.

**In vivo localized <sup>1</sup>H-magnetic resonance spectroscopy:** For liver imaging [14], the 30 mice were treated in the following way. In vivo localized <sup>1</sup>H- Magnetic Resonance Spectroscopy of a liver voxel was performed using A Bruker Micro2.5 gradient system of 1 T/m was used with a solenoidal 30 mm I.D. RF volume coil in transmit/receive mode. Animal placement in the magnet was assessed by three orthogonal slices acquired with a gradient echo protocol (TE 4.0, TR 200 ms, 1 average, FLASH, hermite pulse, 30j, 3.0 cm FOV, 128×128 matrix giving resolution 0.234 mm, slice thickness 1.0 mm, with respiratory triggering). The animal position was adjusted to center the liver in the coil. A second gradient echo protocol (TE 4.0, TR 220 ms, 1 average, FLASH, hermite pulse, 30j, 3.0 cm FOV, 128×128 matrix giving resolution 0.234 mm, slice thickness 0.8 mm, with respiratory triggering) with 6-9×1 mm axial slices transecting the liver was used to localize the voxel of interest. The global shim was optimized manually with a gated single pulse method (90j block pulse excitation, 500 ms repetition time. Global shimming was used as cardiac motion and low signal to noise made localized shimming difficult. Spectra were acquired with a PRESS protocol. Parameters were: TE/TR=50/3000 ms, 256 averages, 0.5 ms hermite pulses, (2.5)<sup>3</sup> mm voxel, 4K FID, 6009.6154 Hz spectral width, no outer volume suppression. Preliminary spectra of 3 scout voxels (2.5 mm cubed, 32 scans) were acquired from apparently homogeneous regions of the liver as seen on the axial gradient echo slices. Voxels were placed near the liver margins to avoid significant blood vessels and to obtain more homogeneous tissue (Figure 2). Spectra from scout voxels were compared for line width and apparent lipid concentration. A voxel with narrow, undistorted line shapes and a representative lipid concentration was chosen. The development of the method for in vivo localized <sup>1</sup>H-MRS in mouse liver is described in van Ginneken [14].



**Figure 2:** Localized *in vivo* <sup>1</sup>H-MRS in a High-Fat diet (HF) induced C57bl6 Insulin Resistant/Type 2 mouse model with repeated triacylglycerol measurements at the same liver voxel in liver tissue of 2.5×2.5×2.5 mm of –among else- the same animal (n=1) so that triacylglycerol accumulation in the liver (=hepatic steatosis) could be followed in time (see also Figure 4 for the successively in time followed spectra in one animal at the same voxel location).

**Assessment of MRS data:** Spectra were Fourier transformed with 10 Hz exponential line broadening and baseline corrected. Spectroscopic evaluation of hepatic steatosis was limited to quantification of two dominant peaks in the MRS spectrum: water at 4.6 ppm and triacylglycerols (TG's) at 1.2 ppm, to calculate the fat/water ratio. This method is based on two assumptions: 1). methylene proton signals estimated by spectroscopy are specific for the total mobile TG fraction; 2). water content is usable as concentration standard. For validation, we measured TG in mice with different degrees of liver fattening using our *in vivo* <sup>1</sup>H MRS protocol [14].

## Experiment 2: Mass spectrometry (LC-MS)

Lipids and free fatty acids (FFA) were analyzed with electrospray LC-MS. Fifty  $\mu$ l of the well mixed freeze dried tissue homogenate carcass powder was mixed with 1000  $\mu$ l IPA containing 4 internal standards (IS: C17:0 lysophosphatidylcholine, di-C12:0 phosphatidylcholine, tri-C17:0 glycerol ester, C17:0 cholesterol ester and heptadecanoic acid (C17:0)). Samples were placed in an ultrasonic bath for 5 minutes. After mixing and centrifugation (10000 rpm for 3 minutes) the supernatant was transferred to autosampler vial. This procedure was followed by injection of 10  $\mu$  on the LC-MS Instrument (Thermo Electron, San Jose, USA).

Lipids were separated on a 150×3.2 mm i.d. C4 Prosphere column (Alltech, USA) using a methanol gradient in 5 mM ammonium acetate and 0.1% formic acid (mobile phase A: 5% methanol, mobile phase B: 90% methanol). The flowrate was 0.4 ml/min and the gradient was as follows: 0-2 min-20%B, 2-3 min-20% to 80%B, 3-15 min-80% to 100%B, 15-25 min-hold 100%B, 25-32 min -condition at 20% B.

The instrument used was a Thermo LTQ equipped with a Thermo Surveyor HPLC pump. Data were acquired by scanning the instrument from m/z 300 to 1200 at a scan rate of approximately 2 scans/s in positive ion ESI mode.

The FFA LC-MS platform employs the same sample and similar HPLC conditions as the lipid method. The ammonium acetate concentration is 2 mM instead of 5 mM and no formic acid was added. The gradient: 0-2 min-30%B, 2-3 min-30% to 70%B, 3-10 min-70% to 100%B, 10-15 min-hold 100%B, 15-20 min-condition at 30% B. Detection of FFA is performed in negative ion ESI mode. Combined the two methods provide (semi)quantitative data for approximately 200 different identified lipids and FFA.

Each extract was injected three times (10  $\mu$ l), once for the LC-MS FFA platform and two times for the LC-MS lipid platform. Furthermore, a quality control (QC) sample was prepared by pooling the samples. The pool was divided into 10  $\mu$ l aliquots that were extracted the same as the study samples. The QC samples were placed at regular intervals in the analysis sequence (one QC after every 10 samples). The QC samples served two purposes. The first is a regular quality control sample to monitor the LC-MS response in time. After the response has been characterized, the QC samples were used as standards of unknown composition to calibrate the data.

In the homogenate of the carcasses the 6 dominant lipid classes observed with these two methods are the lyso-phosphatidylcholines (IS used: C17:0 lyso-phosphatidylcholine), phosphatidylcholines (IS used: di-C12:0 phosphatidylcholine), sphingomyelins (IS used: di-C12:0 phosphatidylcholine), cholesterylestes (IS used: C17:0 cholesterol ester), triglycerides (IS used: tri-C17:0 glycerol ester), and free Fatty acids (IS used: C17:0 FFA). In addition to these lipids, the extracts also contain minor lipids, but these were either not detected (concentration

too low relative to very abundant lipids like phosphatidylcholines and triglycerides) or they were not included in data processing. The LC-MS lipid and LC-MS FFA data were processed using the LC-Quan software (Thermo).

### Experiment 3: Carcass analyses, allometry

After Experiment 1 and 2 were performed we dried the different components from the mouse groups in crucibles with lid (pre-heated at 550°C) a night-over (16 hours) in an incubator (WTC Binder, Tuttlingen/Germany) at 70°C, then drying at 103°C for 24 hours, and measured by weighing after one hour in the desiccator (ISO-6496). Then the same crucible is ashed in a furnace (Heraeus, Germany) for night-over (16 hours) at 550°C and measured by weighing after one hour in the desiccator (ISO-5984).

Furthermore the frozen mouse (at -20°C) were peeled off from skin, head and limbs. So remaining the body-carcass and freeze dried (Dura-Dry™, FTS-systems, Stone Ridge, New York, USA) for 5 days till constant weight. Samples were then grinded in a seef grinder (Retsh-ZM 100, Germany) with a seef of 1.5 cm mesh. Carcass analyses were performed according to ISO-standards (ISO 5983, ISO/DIS 6492; Geneva, Switzerland). They were homogenized and subsequently sampled for energy, protein, dry matter and fat analyses. Protein content was measured according to ISO 5983 (1979). For fat determination freeze dried sub-samples were extracted as described in ISO/DIS 6492 (1996). Subsamples were assessed for energy according to DIN 5900-2 with an IKA Bomb-calorimeter C-700 T IKA (Analysis-technique GmbH, Germany).

### Statistics and Calculations LC-MS Data

For all measured parameters of the carcasses a comparison was made between the three groups using the individual mouse data (Co, 24 hr starvation, 40 days High-fat diet). Statistics were performed via SPSS (Field 2005) using a one-way ANOVA for differences between the three groups.  $P \leq 0.05$  was considered as statistically significant. Normality of the data and homogeneity of variances were checked by Kolmogorov-Smirnov and Fmax tests, respectively.

Principal Component Analysis (PCA) was carried out on the parameters of lipid metabolism measured via reversed phase liquid chromatography coupled to mass spectrometry. This type of analysis allows one to simultaneously examine the relative state of individuals according to three or more variables. We used Principal Component Analysis (PCA) statistical methods, which are specially developed, for application in biomedical research using TNO IMPRESS, EQUEST and WINLIN software [21,22].

Principal components analysis is a classic statistical technique used to reduce multidimensional data sets to lower dimensions for analysis [23]. The applications include exploratory data analysis and data for generating predictive models. PCA involves the computation of the eigenvalue decomposition or singular value decomposition of a data set, usually after mean centering the data for each attribute. The results of a PCA are usually discussed in terms of scores and loadings. The score and loading vectors give a concise and simplified description of the variance present in the dataset [24-28]. A principal component is a linear combination of the original variables (in this case: lipid concentrations) and the magnitude of its eigenvalue is a measure of the explained variance. Typically only a few principal components are required to explain >90% of the total variance in the data. In other words PCA is a dimension reduction method, e.g. from >100 lipid attributes in the data to only a 4 principal components, which simplifies data visualization.

### Results

The Control group (N=6) on the standard chow had an initial body weight of  $27.2 \pm 2.9$  g and increased the Body Weight (BW) in 40 days to  $29.0 \pm 1.7$  g ( $\delta$ -BW: 1.07 g ↑, Figure 3). The High-fat diet group (N=7) increased in body weight in 40 days from  $27.5 \pm 2.3$  g to  $35.4 \pm 5.8$  g ( $\delta$ -BW: 7.9 g ↑, Figure 3). The starvation group (N=7) reduced the Body Weight from  $27.8 \pm 2.4$  g to  $21.8 \pm 1.8$  g after 24 hrs of starvation ( $\delta$ -BW: 6.0 g ↓, Figure 3). For comparison in Table 2 literature data are given which will be discussed in the Discussion paragraph.

In Table 2 (Results experiment 3) the effect of the three nutritional treatments on the biochemical composition of the carcass is given. The following topics can clearly be distinguished. In the High-fat diet group the lipid content of the liver measured with <sup>1</sup>H-MRS (mainly TG) increases after 40 days of a High-fat diet until a value of 5583% compared to the Control group.

Ash (minerals) drops significantly in the Starvation group (compared to Co) until 64%.

Crude protein in the 24 h starvation group, increases significantly, compared to Co and High-fat diet group until 142% and 211%, respectively.

Fat in the carcass increases in the High-fat diet group in comparison with the Control group until 532% while in the 24 h starvation group (in comparison to the Co-group) the fat of the carcass drops significantly until 37%. Furthermore there is a tremendous drop of the carbohydrates in the 24 h starvation group until 5.5% of the Control group. In contrast the carbohydrates in the High-fat diet carcass increases until 154% of the Control value.

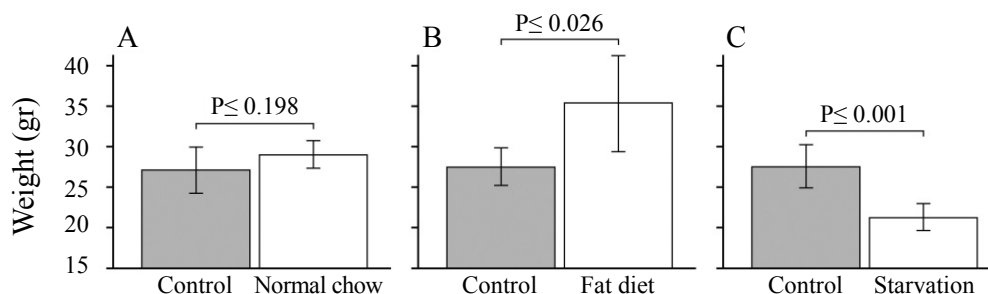


**Figure 3:** The average of bodyweight of A) a control mouse group (N=7) in comparison to the weight after 40 days on standard chow (same group, N=7); B) a control mouse group (N=7) in comparison to the weight after 40 days on a High-fat diet (N=7); C) a control mouse group (N=7) in comparison to a 24 hours starvation group, (N=7).

Compound	Control (A) (Mean ± SD) (n=7)	Starvation (B) (Mean ± SD) (n=7)	Fat (C) (Mean ± SD) (n=7)	Kruskal - Wallis	P-value		
					A vs. B	A vs. C	B vs. C
MRI/fat Dimensionless	0.06 ± 0.04	n.d.	3.35 ± 3.42	0.0258**	-	0.042*	-
Ash (g/kg/dm)	121.9 ± 13.5	78.0 ± 27.8	189.9 ± 19.5	0.2579	0.0003**	0.018*	0.00001***
Crude protein (g/kg/dm)	529.2 ± 50.7	748.7 ± 24.8	354.4 ± 74.8	0.0001***	0.00001***	0.006**	0.00001***
Energy (kJ/g/dm)	24.8 ± 0.70	19.9 ± 1.4	30.2 ± 2.4	0.0001***	0.0001***	0.001**	0.00001***
Fat (g/kg/dm)	297.2 ± 47.2	109.5 ± 43.2	583.0 ± 149.9	0.0001***	0.0003***	0.001**	0.00003***
Carbohydrates (g/kg/dm)	5.4 ± 1.7	0.3 ± 0.6	8.3 ± 2.0	0.0001***	0.0006***	0.046*	0.00001***

**Table 2:** Biochemical composition of the carcass of three mice groups (Control (n=6), 24 h starvation (n=7) and 40 days High-fat diet (n=7). n.d.= not detected.

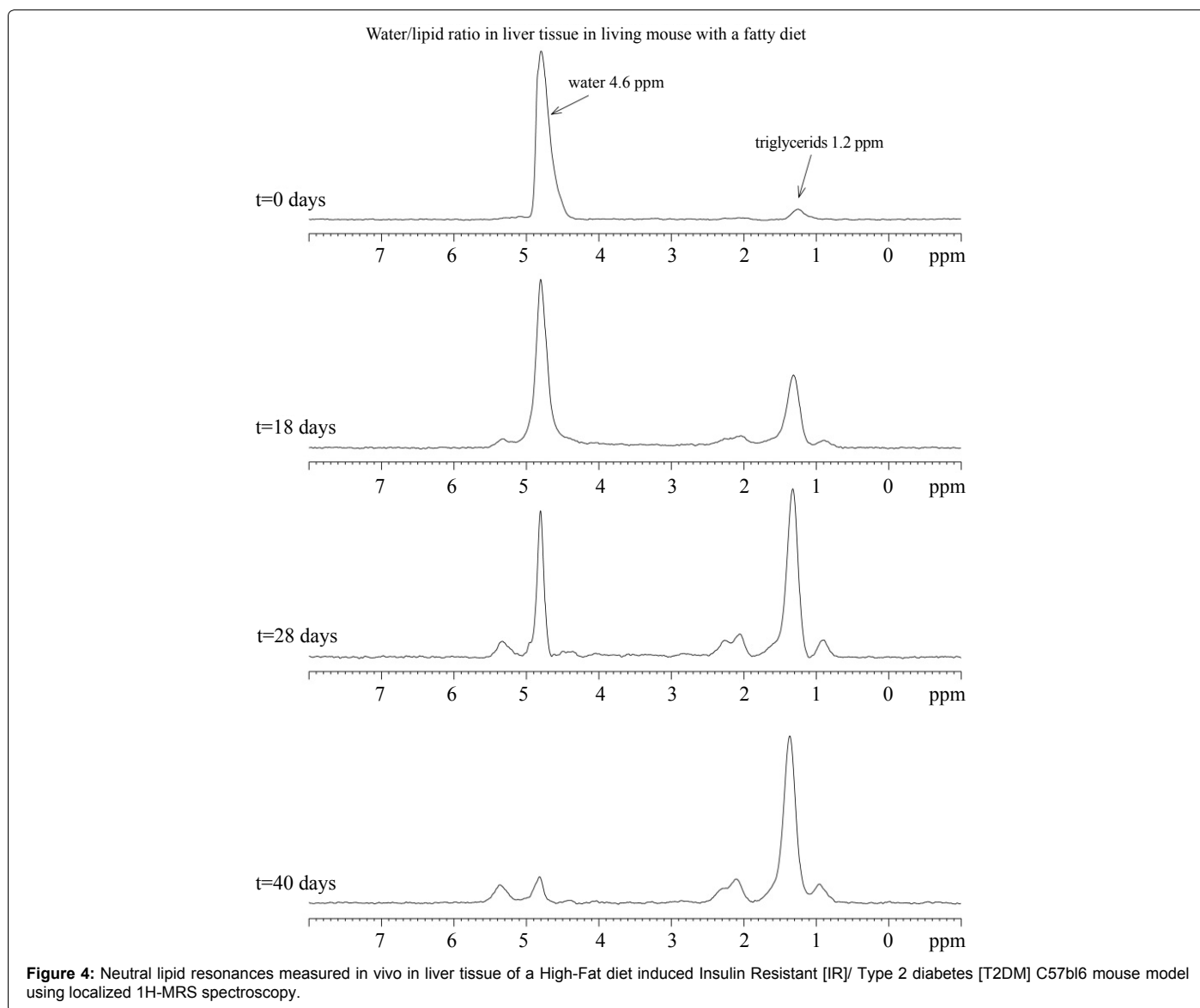


**Figure 4:** Neutral lipid resonances measured in vivo in liver tissue of a High-Fat diet induced Insulin Resistant [IR]/ Type 2 diabetes [T2DM] C57bl6 mouse model using localized <sup>1</sup>H-MRS spectroscopy.

### Experiment 1: <sup>1</sup>H-MRS liver

In Figure 4 the two dominant peaks (water at 4.6 ppm and triacylglycerols at 1.2 ppm) are visualized. This is an example of one animal followed during the period of 40 days on the High-fat diet.

Clearly we see at day 18, 28 and 40 an increase of the triacylglycerol peak (at 1.2 ppm) and a decrease of the water peak (at 4.6 ppm). From this figure it is not clear whether the water/lipid content of the liver changes. Therefore, we determined in experiment 3, (called “allometry” experiment), the dry matter content (g/kg) and ash content (g/kg) for

different body compartments: a). carcass, b). subcutaneous, c). head/legs/tail, d). liver and e) intestine.

Only the water peak at 4.6 ppm and the triacylglycerol (TG) peak at 1.2 ppm are followed in the same animal which is followed for 40 days at a High-fat diet at the same liver voxel location (Figure 2). With the <sup>1</sup>H-MRS technique this animal serves as its own control.

### Experiment 2: LC-MS Chromatogram of the carcasses of the three groups (Control, 24 h starvation, High-fat diet)

The chromatogrammes of the three mouse groups are given in Figures 4 and 5. Several groups of chemical compounds can be clearly distinguished in these figures.

**Retention-times:** MG: monoglycerols 9-11 min; LPC: lysophosphatodol-cholines 9.5-11 min; DG: diacyl-glycerols 11.5-16 min; PC: phosphatodolcholines 13-16 min; PE: phosphatodol-esters 13.5-15 min; SPM: sphingomyelins 13.5-16 min; ChE: cholesterol-esters 17.5-19 min; TG: triacylglycerols 16-20.

### Experiment 2: LC-MS-measurements

The canonical correlation of LC-MS data in this study of lipid analysis of the carcass demonstrates that clearly three groups can be distinguished (Figure 6). So the two diet interventions 24 hours and 40 days. High Fat diet had a clear effect on the lipid analysis of the carcass. Looking at only differences larger than 1000% we see that between the starvation and the fat group the largest differences can be observed for diacylglycerols and triacylglycerols (Annexure 1).

### Experiment 3 (Allometry)

Most important observation of the allometry experiment, given in Table 3, is that there is no significant difference in liver composition for dry matter and ash between the three groups. So the accumulation of the TG measured with localized <sup>1</sup>H-MRS techniques can be ascribed to TG accumulation and not to a different water/lipid content of the liver. In addition, comparing the control group with the High-fat diet group of this murine model the intestines show the largest fat accumulation followed by the head/legs/tail. Surprisingly the subcutaneous fat stores did not change significantly between Control and High-fat diet group. The head/legs/tail remained the same for dry matter and ash between starvation and High-fat diet group.

### Experiment 1 and 3: <sup>1</sup>H MRS of liver (TG) and lipid content of the carcass

For the <sup>1</sup>H MRS measurements we could not handle the 24 hours starvation mice and put them under anaesthesia in the magnet. Therefore Figure 7 is only composed of mice from the Control and High-fat diet group (N=29). The Y-axis gives the triacylglycerol (TG) accumulation in the liver measured with localized <sup>1</sup>H MRS (dimensionless) while the lipid content of the carcass for the corresponding animal is given on the X-axis. The most important observation of this study is that when the muscle compartment is saturated with lipids until  $\approx 500$  g/kg dm there is no TG accumulation in the liver but above this level there is a spill over in the plasma resulting in fat accumulation in the liver.

### Discussion

The effect of the three treatments: 40 days Control Chow diet, 24 hours starvation and 40 days a High-fat diet has a clear effect on the body weight and is given in Figure 1 of the Results paragraph. The described observations of our experimental groups correspond in great

extent with the observations of other authors, given in Table 4, which confirms that our treatments (24 hours starvation and 40 days High-fat diet intervention) were sound.

The pathogenesis of IR/T2DM is complex and some of the factors involved are described in the manuscript by discussing the results of other authors but also our results. High-fat diet feeding results in high plasma insulin levels which stimulates lipoprotein lipase (LPL) that activates the hydrolysis of chylomicron TG and VLDL-TG in blood into Fatty acids, which accumulate in tissues [19,13]. In mammals, the most important lipid store of the body is represented by triacylglycerols (TG's), found mainly in adipose tissue, which is the major site of lipolysis: 10-30% of the body weight is adipose tissue [29]. In addition to adipocytes, the liver and skeletal muscle can accumulate TG, although to a much lesser extent. It is suggested that mismatch between free fatty acid import and utilization resulting in lipid accumulation in organs like heart, skeletal muscle, pancreas, liver and kidney play an important role in the pathogenesis of heart failure [13], obesity and diabetes [12,15].

In addition to FFA that circulate in plasma in increased amounts, increased stores of TG has been observed in muscle in muscle of obese individuals [30,31] and liver [7,14] correlate closely with the presence of Insulin resistance in these tissues. The TG's in liver and muscle are in a state of constant turnover, and the metabolites of intracellular TG lipolysis impair insulin action in both liver and muscle. This effect has been referred to as lipotoxicity [9,12,32]. It is recognised that muscle lipid content in particular intramyocellular lipids (IMCL), correlate better with insulin resistance than plasma FFA [33].

The major message of this manuscript is the interaction of remnant organ/tissue called "carcass" in the absorption capacity of lipids and the spill-over of these lipid compounds (mainly TG's) to the liver. Our data suggest that if the remnant muscle compartment is saturated with lipids until  $\approx 500$  g/kg dm there is no TG accumulation in the liver, but above this level there is a spill over in the plasma resulting in fat accumulation in the liver (Figure 6). The activation of lipolysis is under acute neural and hormonal control [9,14,34].

Other factors which we systematically discuss in this manuscript are the characteristics of other organs like: A). the liver; B) adipocytes; C) peripheral tissue like skeletal muscle; D) Body composition, amount of protein vs. fat; E). Several (toxic)-lipid compounds.

### Liver

In principle there are four sources of High-fat acid accumulation in the liver [35]: 1) the non- esterified Fatty acids (NEFA) pathway: this pathway consist of peripheral fats stored in adipose tissue that flow to the liver; 2). the de novo lipogenesis pathway (DNL): this pathway consist of Fatty acids newly made from 2-carbon precursors (e.g., dietary carbohydrate) within the liver, 3) Plasma derived dietary Fatty acids: these dietary Fatty acids spill over into the plasma NEFA pool, and 4) remnant-derived dietary Fatty acids: these dietary Fatty acids are taken up by intestinally derived chylomicron remnants directly into the liver.

It is assumed that excessive accumulation of fat into the liver is mostly coming from the adipose tissue via the NEFA pool [36]. Subjects with NAFLD, have a moderate increase in post-absorptive NEFA-levels and lypolytic flux and some resistance of lypolysis to the action of insulin. This can probably explain the increased insensitivity of animals to insulin exposed to a High-fat diet. These results indicate an increment of NEFA delivery to the liver in animals without

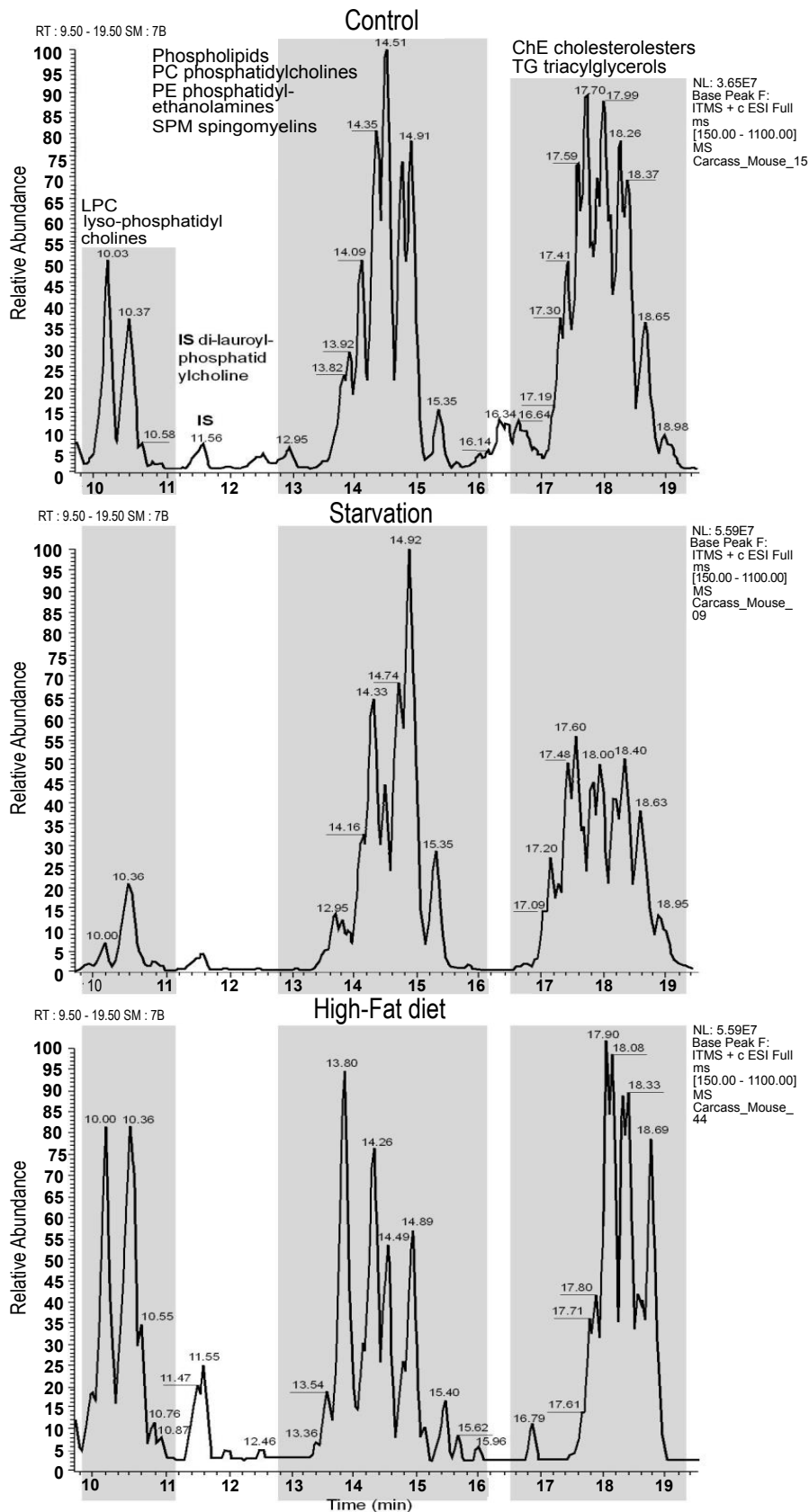
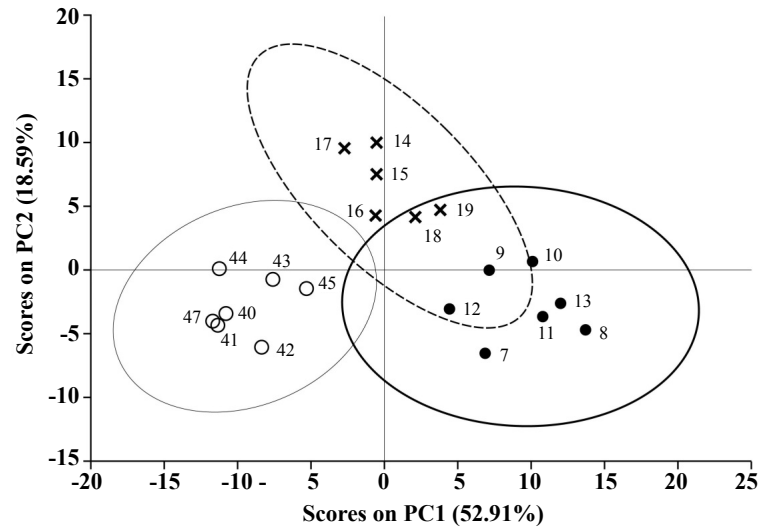


Figure 5: Examples of three chromatogram's of a single mouse given a different diet intervention: A) Control diet (top); B) 24 h starvation group (middle); C) High-fat diet; (bottom).



**Figure 6:** Canonical correlation of LC-MS (ES) data is a study of the lipid analysis in carcass homogenate of a control mouse group (x), one group starved 24 hours (o) and one was exposed for 40 days to a High-fat diet (•). Principal component analysis (PCA) was performed on the lipid components in the carcass homogenate of the three groups. Each data point on the plot represents a separate measurement of metabolites in carcass homogenate with LC-MS techniques on 1 animal.

Compound	Control (A) (Mean ± SD)	Starvation (B) (Mean ± SD)	Fat (C) (Mean ± SD)	Kruskal - Wallis	P-value		
					A vs. B	A vs. C	B vs. C
<b>Dry matter (g/kg)</b>							
<b>Carcass</b>	324.7 ±14.7	282.8±8.8	332.2±6.4	0.0001***	0.0001***	0.2742	0.0001***
<b>Subcutaneous</b>	424.3±38.0	348.0±24.9	459.9±30.4	0.0001***	0.0008***	0.0923	0.0001***
<b>Head/legs/tail</b>	352.1±8.3	338.5±7.5	339.7±6.6	0.0066**	0.0075***	0.0128**	0.7911
<b>Liver</b>	285.0±7.3	278.2±22.5	287.4±16.8	0.5942	0.4660	0.7308	0.4286
<b>Intestine</b>	239.8±14.6	217.0±9.3	376.1±27.6	0.0001***	0.0045**	0.0001***	0.0001***
<b>ASH (g/kg)</b>							
<b>Carcass</b>	37.1±2.2	45.6±2.9	35.3±1.5	0.0001***	0.0001***	0.1077	0.0001***
<b>Subcutaneous</b>	9.0±0.4	9.5±0.5	7.8±0.3	0.0001***	0.0615	0.0001***	0.0001***
<b>Head/legs/tail</b>	65.2±4.1	76.9±4.9	71.9±3.4	0.0003***	0.0004***	0.0084**	0.0587
<b>Liver</b>	13.9±0.5	14.3±0.5	13.7±0.6	0.1128	0.1659	0.4227	0.0592
<b>Intestine</b>	14.1±0.6	17.2±1.3	12.1±0.9	0.0001***	0.0001***	0.0007***	0.0001***

**Table 3:** Allometry: Dry matter content (mean ± SD, g/kg) and Ash (mean ± SD g/kg) of three mice groups (Control (n=6), 24 h starvation (n=7) and 40 days High-fat diet (n=7)).

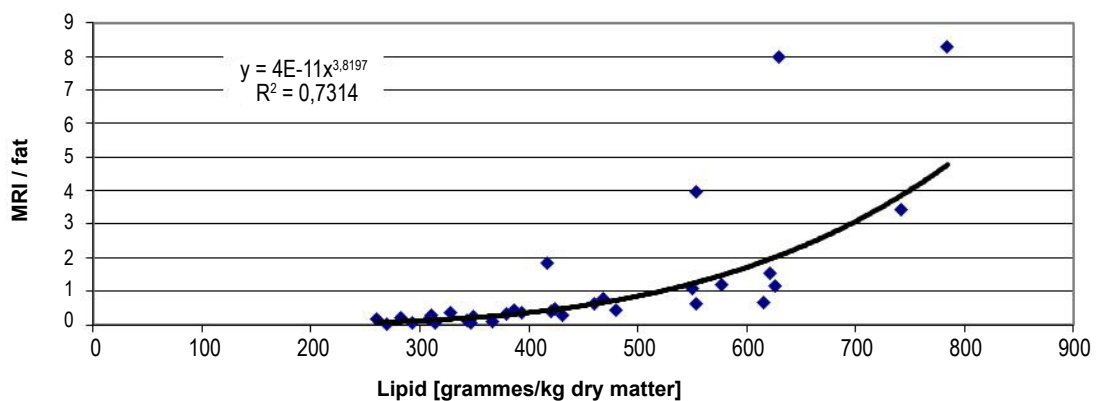


**Figure 7:** Relation between TG concentration measured by 1H MRS and lipid content of the carcass (N=29).

gluconeogenesis (amino acids, lipids and other carbohydrates are transformed into glucose). So the liver keeps the glucose concentrations as steady as possible.

Another way in which there will be accumulation of TG's in the liver is via de novo lipogenesis (DNL). This last pathway will increase, but the NEFA pool will remain the most important source of TG's stored in the liver [36].

NO	Species	Condition	Observation	Author
1	Mice, C57bl/6	16 h starvation	11.1 % reduction B.W	[24]
2	Mice (Swiss albino)	48 h starvation	21.0 % reduction B.W.	[25]
3	Rat (Sprague-Dawley)	48 h starvation	23.0 % reduction B.W.	[25]
4	Mice, C57bl/6	24 starvation	21.6 % reduction B.W.	This study
5	Mice, C57bl/6	8 weeks High-fat diet	11.4% increase B.W.	[26]
6	Mice, C57bl/6	15 weeks High-fat diet	23.1% increase B.W.	[26]
7	Mice, C57bl/6	19 weeks High-fat diet	30.5% increase B.W.	[26]
8	Mice, C57bl/6	9 weeks High-fat diet	30.4% increase B.W.	[27]
9	Mice, C57bl/6	12 weeks normal chow	3.5% increase B.W.	[28]
10	Mice, C57bl/6	12 weeks High-fat diet	39% increase B.W.	[28]
11	Mice, C57bl/6	40 days normal chow	6.6% increase B.W.	This study
12	Mice, C57bl/6	40 days High-fat diet	28.7% increase B.W.	This study

**Table 4:** Literature overview of starvation or diet intervention (normal chow vs. High-fat diet) in different mice and rat strains.

However, apart from fat accumulation from adipose tissue via the NEFA pool our study demonstrates a little described route of TG accumulation in the liver originating from muscle tissue. The control of non-adipose stores in e.g. muscle tissue is poorly documented [26]. Increased plasma FFA's leads to intramyocellular lipid accumulation in humans that has been proposed to play a critical role in the genesis of insulin resistance (IR) and type 2 diabetes [15]. Intramyocellular lipid accumulation is associated with activation of protein kinase-C (PKC) [37]. Alterations in PKC activation may interfere with normal insulin signaling.

### Adipocytes

Koska et al. [38] gave in their introduction an excellent review of the enlargement of subcutaneous human adipocytes, which leads may in turn lead to increased accumulation of fat in visceral adipose tissue, skeletal muscle, and liver and a subsequent worsening of insulin action and glucose tolerance. They describe that the mechanism underlying abnormal partitioning of lipids in hypertrophic obesity, and metabolic derangements reminiscent of those seen in lipodystrophic syndromes, may involve other factors in addition to simple overflow of fat from large dysfunctional adipocytes, an suggest that one such factor may be the adipocyte-derived, insulin-sensitizing hormone adiponectin [38].

In addition, "adipocytes" is just a general term for different adipose stores. E.g. if we consider for rodents only the adipose tissue there are in principle four adipose pools: retroperitoneal, epididymal, mesenteric and subcutaneous [17].

### Muscle and heart

Three causes for ectopic fat storage (in tissues other than adipocytes like peripheral tissue like muscle and heart) can be mentioned. First, insufficient adipose tissue mass leads to enlarged fat cells and to excess energy storage as TG in liver and skeletal muscle. The sequence of events by which the inability to store fat in adipose tissue leads to ectopic accumulation of TG in muscle and liver, hepatic and muscle insulin resistance, glucose intolerance, and overt diabetes has been referred to as "the overflow hypothesis". The "overflow hypothesis" also explains the observation that enlarged fat cells correlate better with insulin resistance than any other measure of adiposity [32], and one could therefore argue that "the overflow hypothesis" should no longer be considered hypothetical.

The second mechanism that can cause fat storage in other tissues than adipose tissue is a failure of fat cell proliferation and/or differentiation [39]. The control mechanisms for adipocyte differentiation are complex and different transcription factors, which in turn are regulated in response to extracellular signals, are involved

[14]. Defects in any one of these steps are potentially important in the failure of proliferation or differentiation of adipocytes [39]. Finally, the third mechanism that can cause ectopic fat storage is that whole-body fat oxidation is impaired. In this view the machinery to oxidise fat is not sufficient to match the dietary fat load or is not activated in a timely fashion by a signal necessary to oxidise fat.

### Body composition, amount of protein vs. fat

The influence of body composition on partitioning of production energy also has consequences for the "protein deposition capacity" of mice. Capacity is defined here as the protein deposition rate at ideal nutritional circumstances [40]. An animal which is relatively fat (due to nutritional manipulation) can, compared to a less fat animal, put a lower preference towards protein deposition. This because we found a negative regression between fat accumulation in the carcass in relation to protein deposition capacity (Table 5,  $R_2=0.946$ ).

The deposition of excess fat is accompanied by a decrease in the fat-free component-protein, ash and water (Table 5, fat-protein  $R_2=0.946$ ; ash-lipid  $R_2=0.914$ ). This observation suggests that obesity susceptible strains may be characterized not only by excessive fat deposition but also by lower rates of protein synthesis or higher rates of protein degradation. Replacement of protein's in the muscle by fats might result in "Sacropenic obesity" [41], a condition which is closely related to obesity-associated Insulin resistance and Dysglycemia [42]. Increased protein intake is positively correlated with and can bolster, growth hormone (somatropin) production, [43], IGF-1 [44], and glucagon [45]. These hormones, collectively, exert an anabolic and lipolytic effect. Especially, somatropin is a powerful lipolytic- (fat mobilizing) [46], anabolic- (muscle-enhancing) [47], immune system stimulating hormone [48] that also directly influences cholesterol and triacylglycerol levels [49]. Protein also exerts a weak stimulatory effect on insulin, approximately 30% of the effect of carbohydrate on insulin [50]. So replacement of protein in the muscle by a High-fat diet may result in an opposite effect as described in the paragraph above and result in a decline of the anabolic/catabolic hormone-axis and an increase of the lipogenic/lipolytic hormone axis which can explain extremely high correlation ( $R_2$ ) found between the different measured (experiment 3) body components given in Table 5.

### Several (toxic)-lipid compounds

High-fat feeding leads to the development of dietary obesity, but not only the amount but also the fatty acid composition of dietary lipids are relevant. Indeed, much evidence has now been found that the nature of the dietary fats can affect lipid homeostasis and body fat accumulation. For instance, feeding fish oil selectively reduces the hypertrophy of

Y-axis	X-Axis	Equation	R <sup>2</sup>
MRI-TG	Energy kJ/g dm	Y=3E-17x <sup>11.276</sup>	0.719
MRI-TG	Lipid g/kg dm	Y=4E-11x <sup>3.8197</sup>	0.731
Ash g/kg dm	Crude Protein g/kg dm	Y=0.2868x-27.117	0.951
Ash g/kg dm	Energy kJ/g dm	Y=-10.448x + 393.48	0.922
Ash g/kg dm	Lipid g/kg dm	Y=-0.226x + 207.44	0.914
Lipid g/kg dm	Crude Protein g/kg dm	Y=-1.2052x + 1006.5	0.946
Lipid g/kg dm	Energy kJ/g dm	Y=43.982x-764.87	0.913
Crude Protein g/kg dm	Energy kJ/g dm	Y=-36.065x+1457.8	0.947

**Table 5:** We can conclude that the ability of linear measurements to give correlations between body composition (fat free mass: ash, protein and water) under conditions of starvation, control or High-fat diet has proven, considering the high correlation coefficients, to be a suitable method.

Compound	Control (A) (Mean ± SD)	Starvation (B) (Mean ± SD)	Fat (C) (Mean ± SD)	Kruskal - Wallis	P-value			Change in %		
					A vs. B	A vs. C	B vs. C	A vs. B	A vs. C	B vs. C
<b>C16-0-SPM</b>	0.313 ± 0.015	0.249 ± 0.065	0.289 ± 0.061	0.161	0.3790	*0.0400	0.2966	92.39	79.59	86.14
<b>C18-0-SPM</b>	0.480 ± 0.034	0.315 ± 0.069	0.375 ± 0.065	**0.003	**0.0056	***0.004	0.1548	78.06	65.67	84.13
<b>C18-3-SPM</b>	0.038 ± 0.003	0.029 ± 0.006	0.043 ± 0.009	*0.017	0.2098	*0.0121	*0.0122	114.37	77.28	67.57
<b>C22-0-SPM</b>	0.211 ± 0.021	0.164 ± 0.051	0.240 ± 0.072	0.118	0.3703	0.0638	0.0622	113.68	77.86	68.49
<b>C23-0-SPM</b>	0.066 ± 0.009	0.041 ± 0.009	0.058 ± 0.014	*0.017	0.2411	***0.006	*0.0310	87.29	61.54	70.50
<b>C24-0-SPM</b>	0.237 ± 0.019	0.108 ± 0.040	0.263 ± 0.079	**0.003	0.4520	***0.000	**0.0016	110.94	45.53	41.04
<b>C24-1-SPM</b>	0.392 ± 0.020	0.330 ± 0.109	0.487 ± 0.139	0.224	0.1282	0.2010	0.0544	124.36	84.21	67.71

**Table 6:** Changes in sphingomyelin (SPM) values, the precursor of the toxic compound ceramide in the pathogenesis of Insulin resistance and/or Type-2 diabetes (IR/T2DM) Experimental set up and LC-MS measurements were performed as described in Material and Methods.

retroperitoneal and epididymal adipose tissue in rate compared with a diet containing the same amount of lard in conditions of similar energy intake [51,52]. The LC-MS data of this study indicate that the fatty acid composition of non-adipose tissue is markedly affected by dietary fats. The relationships between the molecular structure of fatty acids and their relative mobilization are strongly analogous to those between their structure and their retention time on non-polar GLC columns. This suggests that the differential mobilization is related to a differential solubility of fatty acids, perhaps in water at the lipid-water interface where hormone-sensitive lipase hydrolyses triacylglycerols (TG's). Therefore this study was extended using LC-MS techniques on the lipid compounds of the carcass in three mice groups: starvation, control and overfeeding. The differential mobilization of fatty acids could markedly influence the storage of individual fatty acids in adipose tissue, and their utilization and supply to tissues and organs when lipolysis is enhanced, e.g. during overfeeding. Although not the main objective of this study (and therefore not presented in the paragraph "Results"), a second consequence of the delivery of lipids to peripheral tissues in excess of their oxidative or storage capacities is lipotoxicity, caused by toxic conversion products like e.g. sphingomyelin (SPM) and ceramide [53,54]. SPM is a sphingolipid, located mostly in the outer layer of the plasma membrane. Ceramide is the second messenger in the sphingomyelin signaling pathway. Experimental studies revealed that ceramide might impair insulin action via: 1) maintaining protein kinase B in an inactive dephosphorylated state, 2) a reduction of GLUT4 translocation to plasma membrane, 3) a decrease in insulin-stimulated glucose uptake, 4) Tumor Necrosis Factor (TNF)-α, a well-known mediator of insulin resistance, acts through activation of neutral shingomyelinase (enzyme which hydrolysis sphingomyelin => ceramide) and induction of ceramide formation [54]. At the moment we performed the LC-MS measurements we were unable to measure ceramide but only its precursor SPM. To make optimal use of the in this study gathered information we can have a quick glance which SPM are increased due in remnant muscle of this black six mouse after exposure for 40 days to a High-fat diet. If we look at Table 6 there are significant

changes in by LC-MS techniques SPM values between Control- and High-fat exposed mouse groups but they are only indicative for a decline in the range between 46-84% of the initial Control value. Therefore we can assume that the SPM=>ceramide conversion may not play a role for remnant muscle ("carcass") in the pathogenesis of IR/T2DM.

### Coming back to the major observations of our study

Allometry observations from this mice experiment gave two important observations:

First, there is no significant difference in liver composition for dry matter and ash between the three groups. So the accumulation of the TG measured with localized <sup>1</sup>H-MRS techniques can be ascribed to TG accumulation and not to a different water/lipid content of the liver. Secondly, fat accumulation is tissue dependent because if we compare the Control group with the High-fat diet group of this mice model the intestines show the largest fat accumulation followed by the head/legs/tail. Surprisingly the subcutaneous fat stores did not change significantly between Control and High-fat diet group.

We used the ratio of the methylene peak to the water in the MRI in order to quantify the fat accumulation. One of the stated assumptions is that the water content can be used as a concentration standard. Lipid is primarily stored in large vesicles in the liver and given the hydrophobic content of the vesicles it is reasonable to assume that the water content of lipid filled vesicles is much less than the water content of the surrounding liver. Thus as a liver fills up with fat, the water content per unit volume will decrease. This will lead to significant non-linearity in the ratio. In order to test this hypothesis and test that the water concentration remains constant at all levels of lipid accumulation in the liver we performed allometry and measured in a parallel experiment dry matter and ash content in 5 body compartments: a). carcass, b). skin and subcutaneous fat, c). head legs and tail, d). liver, e). intestine and abdomen; in the three mice groups (control, 24 starvation, 40 days

High-fat diet). The results demonstrate that carcass, subcutaneous fat store and abdomen are much affected, but not the liver. So the water concentration remains constant at all levels of lipid accumulation in the liver.

## Conclusion

So we demonstrated in this manuscript that the “cross-talk” [6], between tissues/organs suited for fat storage like liver [35] and adipocytes [38] but also peripheral tissues not suited for lipid storage like heart- and skeletal muscle [12,15], can be extended with another body/tissue compartment namely non-adipose remnant tissue/muscle ≈ “carcass”, like we proved in this manuscript.

## Acknowledgements

Experiments were supported by a grant of Center for Medical Systems Biology (CMSB), Leiden University.

## References

- Ashcroft FM, Ashcroft SJH (1992) *Insulin: molecular biology to pathology*, Oxford University Press, USA.
- Baynes J, Dominiczak M (2004) Glucose homeostasis and fuel metabolism. *Med Biochem* 2: 243-266.
- Cohen CY (1987) Energy metabolism in the brain, adaptation towards starvation. *Med Hypotheses* 24: 177-178.
- Wallberg-Henriksson H (1986) Glucose transport into skeletal muscle. Influence of contractile activity, insulin, catecholamines and diabetes mellitus. *Acta Physiol Scand Suppl* 564: 1-80.
- Salway JG (2004) Metabolism at a glance. *Metab a Glance*.
- Taylor SI (1999) Deconstructing type 2 diabetes. *Cell* 97: 9-12.
- van Ginneken V (2008) Liver fattening during feast and famine: an evolutionary paradox. *Med Hypotheses* 70: 924-928.
- van Ginneken V, Verhey E, Poelmann R, Ramakers R, van Dijk KW, et al. (2007) Metabolomics (liver and blood profiling) in a mouse model in response to fasting: A study of hepatic steatosis. *Biochim. Biophys. Acta - Mol Cell Biol Lipids* 1771: 1263-1270.
- van Ginneken V, Feskens E, Poelmann RE (2010) Review: Insulin Resistance: Intra-uterine growth retardation, life style, genetic susceptibility, prevention and treatment. *Adv Med Biol Res*, Nova Science Publishers.
- Randle PJ, Garland PB, Hales CN, Newsholme EA (1963) The glucose fatty-acid cycle its role in insulin sensitivity and the metabolic disturbances of diabetes mellitus. *Lancet* 281: 785-789.
- Phielix E, Mensink M (2008) Type 2 diabetes mellitus and skeletal muscle metabolic function. *Physiol Behav* 94: 252-258.
- Chavez JA, Summers SA (2010) Lipid oversupply, selective insulin resistance, and lipotoxicity: molecular mechanisms. *Biochim. Biophys. Acta (BBA)-Molecular Cell Biol. Lipids* 1801: 252-265.
- van Ginneken V, de Vries E, Verheij E, van der Greef J (2016) Metabolomics in Hind limb and Heart Muscle of a Mouse Model after a High-fat Diet. *Anat Physiol* 6: 214.
- van Ginneken V, Verheij E, Hekman M, Greef J, Feskens EJM, et al. (2011) The comparison of lipid profiling in mouse brain and liver after starvation and a high-fat diet: A medical systems biology approach p: 151-186.
- Schaffer JE (2003) Lipotoxicity: when tissues overeat. *Curr Opin Lipidol* 14: 281-287.
- Brown MS, Goldstein JL (2008) Selective versus total insulin resistance: a pathogenic paradox. *Cell Metab* 7: 95-96.
- Raclot T, Mioskowski E, Bach AC, Groscolas R (1995) Selectivity of fatty acid mobilization: a general metabolic feature of adipose tissue. *Am J Physiol* 269: R1060-1067.
- Selman C, Lumsden S, Banger L, Hill WG, Speakman JR (2001) Resting metabolic rate and morphology in mice (*Mus musculus*) selected for high and low food intake. *J Exp Biol* 204: 777-784.
- den Boer M, Voshol PJ, Kuipers F, Havekes LM, Romijn JA (2004) Hepatic steatosis: a mediator of the metabolic syndrome. Lessons from animal models. *Arterioscler Thromb Vasc Biol* 24: 644-649.
- Fawcett (2012) Guideline 22 Guidelines for the Housing of Mice in Scientific Institutions Table of Contents. *ARRP Guidel* pp: 1-143.
- van der Greef J, Davidov J, Verheij E, Vogels J, van der Heijden R (2003) The role of metabolomics in systems biology, in: *Metab. Profiling Its Role Biomark. Discov. Gene Funct Anal* pp: 171-198.
- van der Greef J, van der Heijden R, Verheij ER (2004) The Role of Mass Spectro-metry in Systems Biology: Data Processing and Identification Strategies in Metabolo-mics, in: G.B.A.E. Ashcroft, J.J. Monaghan (Eds.), *Adv. Mass Spectrom.*, Amsterdam: Elsevier Science.
- Jackson DA (1994) Stopping rules in principal components analysis: A comparison of heuristical and statistical approaches. *Ecology* 74: 2204-2214.
- Heijboer AC, Donga E, Voshol PJ, Dang ZC, Havekes LM (2005) Sixteen hours of fasting differentially affects hepatic and muscle insulin sensitivity in mice. *J Lipid Res* 46: 582-588.
- Menahan LA, Sobocinski KA (1983) Comparison of carbohydrate and lipid metabolism in mice and rats during fasting. *Comp Biochem Physiol B* 74: 859-864.
- Lin KC, Cross HR, Smith SB (1992) Esterification of fatty acids by bovine intramuscular and subcutaneous adipose tissues. *Lipids* 27: 111-116.
- Deng Q, She H, Cheng JH, French SW, Koop DR, et al. (2005) Steatohepatitis induced by intragastric overfeeding in mice. *Hepatology* 42: 905-914.
- Johnston SL, Souter DM, Talkamp BJ, Gordon IJ, Illius AW, et al. (2007) Intake compensates for resting metabolic rate variation in female C57BL/6J mice fed high-fat diets. *Obesity (Silver Spring)* 15: 600-606.
- Steinberg D (1963) Fatty acid mobilization--mechanisms of regulation and metabolic consequences. *Biochem Soc Symp* 24: 111-143.
- Itani SI, Ruderman NB, Schmieder F, Boden G (2002) Lipid-induced insulin resistance in human muscle is associated with changes in diacylglycerol, protein kinase C, and IκappaB-α. *Diabetes* 51: 2005-2011.
- Hulver MW, Dohm GL (2004) The molecular mechanism linking muscle fat accumulation to insulin resistance. *Proc Nutr Soc* 63: 375-380.
- Bays H, Mandarino L, Defronzo RA (2004) Role of the adipocyte, free fatty acids, and ectopic fat in pathogenesis of type 2 diabetes mellitus: peroxisomal proliferator-activated receptor agonists provide a rational therapeutic approach. *J Clin Endocrinol Metab* 89: 463-478.
- Assimacopoulos-Jeannet F (2004) Fat storage in pancreas and in insulin-sensitive tissues in pathogenesis of type 2 diabetes. *Int J Obes Relat Metab Disord* 28: S53-57.
- van Ginneken V, Feskens EJM (2010) Epidemiology of Hunger in the World, the Hunger-Obesity Paradox; its Physiological and Endocrinological mechanisms, in: T.C. Merkin Edn, *Biol Starvation Humans Other Org*, Nova Science Publishers, Inc.
- Donnelly KL, Smith CI, Schwarzenberg SJ, Jessurun J, Boldt MD, et al. (2005) Sources of fatty acids stored in liver and secreted via lipoproteins in patients with nonalcoholic fatty liver disease. *J Clin Invest* 115: 1343-1351.
- Tamura S, Shimomura I (2005) Contribution of adipose tissue and de novo lipogenesis to nonalcoholic fatty liver disease. *J Clin Invest* 115: 1139-1142.
- Griffin ME, Marcucci MJ, Cline GW, Bell K, Barucci N, et al. (1999) Free fatty acid-induced insulin resistance is associated with activation of protein kinase C theta and alterations in the insulin signaling cascade. *Diabetes* 48: 1270-1274.
- Koska J, Stefan N, Permana PA, Weyer C, Sonoda M, et al. (2008) Increased fat accumulation in liver may link insulin resistance with subcutaneous abdominal adipocyte enlargement, visceral adiposity, and hypoadiponectinemia in obese individuals. *Am J Clin Nutr* 87: 295-302.
- Heilbronn L, Smith SR, Ravussin E (2004) Failure of fat cell proliferation, mitochondrial function and fat oxidation results in ectopic fat storage, insulin resistance and type II diabetes mellitus. *Int J Obes Relat Metab Disord* 28: 12-21.
- Whittemore CT, Green DM, Knap PW (2001) Technical review of the energy and protein requirements of growing pigs: protein. *Anim Sci* 73: 363-374.
- Stenholm S, Harris TB, Rantanen T, Visser M, Kritchevsky SB, et al. (2008)

- Sarcopenic obesity: definition, cause and consequences. *Curr Opin Clin Nutr Metab Care* 11: 693-700.
42. Srikanthan P, Hevener AL, Karlamangla AS (2010) Sarcopenia exacerbates obesity-associated insulin resistance and dysglycemia: findings from the National Health and Nutrition Examination Survey III. *PLoS One* 5: e10805.
43. Isidori A, Lo Monaco A, Cappa M (1981) A study of growth hormone release in man after oral administration of amino acids. *Curr Med Res Opin* 7: 475-481.
44. Clemmons DR, Underwood LE, Dickerson RN, Brown RO, Hak LJ, et al. (1985) Use of plasma somatomedin-C/insulin-like growth factor I measurements to monitor the response to nutritional repletion in malnourished patients. *Am J Clin Nutr* 41: 191-198.
45. Schmid R, Schulte-Frohlinde E, Schusdziarra V, Neubauer J, Stegmann M, et al. (1992) Contribution of postprandial amino acid levels to stimulation of insulin, glucagon, and pancreatic polypeptide in humans. *Pancreas* 7: 698-704.
46. Piatti PM, Monti LD, Caumo A, Conti M, Magni F, et al. (1999) Mediation of the hepatic effects of growth hormone by its lipolytic activity. *J Clin Endocrinol Metab* 84: 1658-1663.
47. Johansson AG, Engström BE, Ljunghall S, Karlsson FA, Burman P (1999) Gender differences in the effects of long term growth hormone (GH) treatment on bone in adults with GH deficiency. *J Clin Endocrinol Metab* 84: 2002-2007.
48. Auernhammer CJ, Strasburger CJ (1995) Effects of growth hormone and insulin-like growth factor I on the immune system. *Eur J Endocrinol* 133: 635-645.
49. Vahl N, Klausen I, Christiansen JS, Jørgensen JO (1999) Growth hormone (GH) status is an independent determinant of serum levels of cholesterol and triglycerides in healthy adults. *Clin Endocrinol (Oxf)* 51: 309-316.
50. Westphal SA, Gannon MC, Nuttall FQ (1990) Metabolic response to glucose ingested with various amounts of protein. *Am J Clin Nutr* 52: 267-272.
51. Parrish CC, Pathy DA, Parkes JG, Angel A (1991) Dietary fish oils modify adipocyte structure and function. *J Cell Physiol* 148: 493-502.
52. Raclot T (2003) Selective mobilization of fatty acids from adipose tissue triacylglycerols. *Prog Lipid Res* 42: 257-288.
53. Dobrzyń A, Górski J (2002) Ceramides and sphingomyelins in skeletal muscles of the rat: content and composition. Effect of prolonged exercise. *Am J Physiol Endocrinol Metab* 282: 277-285.
54. Straczkowski M, Kowalska I, Nikolajuk A, Dzienis-Straczkowska S, Kinalska I, et al. (2004) Relationship between insulin sensitivity and sphingomyelin signaling pathway in human skeletal muscle. *Diabetes* 53: 1215-1221.